

Latency Modeling of Hyperledger Fabric for Blockchain-enabled IoT Networks

Sungho Lee, Minsu Kim, Jemin Lee, *Member, IEEE*, Ruei-Hau Hsu, *Member, IEEE*,
Min-Soo Kim, and Tony Q. S. Quek, *Fellow, IEEE*

Abstract—Hyperledger Fabric (HLF), one of the most popular private blockchain platforms, has recently received attention for blockchain-enabled Internet of things (BC-IoT) networks. However, for IoT devices handling latency-critical tasks, the additional time spent in HLF has emerged as a new challenge in BC-IoT networks. In this paper, therefore, we develop an HLF latency model using the probability distribution fitting method for HLF-based IoT networks. We first explain the architecture and the transaction flow in HLF, and structure of an HLF-based IoT network. After implementing real HLF, we capture the latencies that each transaction experiences for various HLF environments, and then show that the total latency of HLF can be modeled as a Gamma distribution. Our HLF latency model is also validated by conducting a goodness-of-fit test, i.e., KS test. Furthermore, we explore the impacts of three HLF parameters including transaction generation rate, block size, and block-generation timeout on the HLF latency. As a result, some HLF design insights on minimizing the latency are provided for HLF-based IoT networks.

I. INTRODUCTION

Blockchain technology has been widely studied since the first paper on Bitcoin [1] was presented to propose a monetary system, which provides new solutions to two conventional problems of distributed systems, i.e., data integrity and data consistency [2]. In other words, the blockchain technology enables reliable and secure data management by consensus without a central authority [3]. As a result, many blockchain-enabled applications have emerged in recent years. Particularly, a blockchain-enabled Internet of things (BC-IoT) network has been in the spotlight for IoT data management and security. The BC-IoT network refers to an IoT network, in

which delivered IoT data is appended to the assigned remote blockchain storage. For instance, the information of legitimate IoT devices can be registered in the blockchain storage for authentication [4], and IoT data can be retained and exploited for other applications without data integrity violations [5].

Blockchains can be classified into two types: public blockchain and private blockchain. The private blockchain is considered to be more suitable for the BC-IoT network in terms of faster transaction processing and privacy preservation [6] [7]. Additionally, proof-of-work (PoW), which is usually used in public blockchains like Bitcoin [1], is currently the most popular and general choice for the consensus method. However, PoW is fairly power-consuming because it is mandatory for miners to continuously solve hash puzzles to produce new blocks. Hence, PoW is considered to be unsuitable for power-constrained IoT devices [8]. In contrast, Hyperledger Fabric (HLF), which is one of the most popular private blockchains, supports several alternative consensus protocols without burdening IoT devices in terms of power consumption and computation. This facilitates HLF to work as underlying blockchains in a various range of IoT scenarios and applications. For example, a healthcare system for smart hospitals is proposed to monitor patient vital signs based on HLF [9]. HLF is also utilized to ensure data integrity for sensing data in an integrated IoT blockchain platform [10]. Besides, HLF is employed for trusted wireless monitoring over narrowband IoT networks [11].

However, from the viewpoint of an IoT application that handles real-time jobs, it is important not only to fulfill security requirements using HLF, but also to consider the time consumed in HLF [12]–[14]. Otherwise, they may fail to accomplish latency-critical tasks in a timely fashion. In this sense, it is required to predict and estimate the HLF latency as much as possible, prior to the practical implementation. Unfortunately, however, the HLF latency is quite random, and its statistics have not appeared, which hinders this problem to be resolved. To be specific, HLF has a sophisticated structure, in which many network components simultaneously affect the HLF latency. Thus, it is difficult not only to predict the HLF latency, but also to design HLF with lower latency. Due to this, empirical performance evaluation may be conducted, but it is hard to prepare a precise HLF testbed for every use case of IoT scenarios. Therefore, an HLF latency model is a necessary prerequisite for forecasting and minimizing the HLF latency.

In this paper, therefore, we establish a latency model of HLF especially for HLF-enabled IoT networks, in which time-sensitive data is generally managed. We then consider three

Corresponding author is J. Lee.

S. Lee is with Daegu Gyeongbuk Institute of Science and Technology (DGIST), 333, Techno Jungang-daero, Dalseong-gun, Daegu, Republic of Korea 42988 (e-mail: seuho2003@dgist.ac.kr).

M. Kim was with the Department of Information and Communication Engineering (ICE), DGIST, Daegu 42998, Republic of Korea. He is now with the Wireless@VT Group, Bradley Department of Electrical and Computer Engineering, Virginia Tech, Blacksburg, VA 24061 USA (e-mail: msukim@vt.edu)

J. Lee was with the Department of Information and Communication Engineering (ICE), DGIST, Daegu 42998, Republic of Korea. She is now with the Department of Electrical and Computer Engineering, Sungkyunkwan University (SKKU), Suwon 16419, Republic of Korea (e-mail: jemin.lee@skku.edu).

R.-H. Hsu is with National Sun Yat-sen University, 70 Lienhai Rd., Kaohsiung 80424, Taiwan, R.O.C. (e-mail: rhhhsu@mail.cse.nsysu.edu.tw).

M.-S. Kim is with Korea Advanced Institute of Science and Technology (KAIST), 291, Daehak-ro, Yuseong-gu, Daejeon, Republic of Korea 34141 (e-mail: minsoo.k@kaist.ac.kr).

T. Q. S. Quek is with Information Systems Technology and Design Pillar, Singapore University of Technology and Design, Singapore 487372 (e-mail: tonyquek@sutd.edu.sg).

important HLF parameters, i.e., block size, block-generation timeout, and transaction generation rate, and analyze their impacts on the HLF latency. The contributions of this paper are listed as follows:

- We develop the latency model of HLF v1.3, which has a new structure consisting of transaction-processing stages and is also adopted in the latest HLF releases. Hence, our work is more relevant and appropriate for current HLF-enabled IoT networks, compared to the previous studies on HLF v0.6.
- We provide the probability distribution of the total latency of HLF by performing the probability distribution fitting method on transaction latency samples, which are captured in HLF v1.3. We provide our fitting results with the values of corresponding probability distribution parameters for various HLF parameter setups. To the best of our knowledge, this is the first work that provides the distribution of the HLF latency.
- We explore the impacts of three main HLF parameters, i.e., block size, block-generation timeout, and transaction generation rate, on the HLF latency. Especially, we figure out the existence of the best values of those HLF parameters that minimize the HLF latency. This provides some insights on the design of HLF parameters to lower the HLF latency in BC-IoT networks.

The remainder of this paper is organized as follows. In Section II, we discuss previous studies on HLF performance evaluation and modeling with their limitations. We provide a brief overview of HLF and describe HLF-enabled IoT networks in Section II. We then provision our HLF latency model based on probability distribution fitting in Section IV. In Section V, we analyze the impacts of the important parameters aforementioned on the HLF latency, and then explore the methods for minimizing the mean HLF latency. Lastly, the conclusions of this paper are summarized in Section VI.

II. RELATED WORK

In this section, we present related work on HLF performance evaluation and modeling, then discuss limitations discovered in literature.

A. HLF Performance Evaluation

The HLF performance evaluation work is to observe and evaluate HLF performance in various HLF setups or scenarios on HLF v0.6 [15]–[17] or on HLF v1.0 or higher [18]–[23]. The throughput and latency of HLF v0.6 are compared to those of other private blockchain platforms, such as Ethereum and Parity, in [15] and [16]. In [15], a private blockchain benchmarking framework is developed and exploited for their observations. In [16], network congestion in HLF v0.6 and Ethereum from varying workloads is considered. For the consensus method, HLF v0.6 provides practical Byzantine fault tolerance (PBFT) only, which is not currently available in HLF v1.0 or higher. The performance of PBFT is evaluated in [17], especially when malicious nodes attempt to subvert the network.

In a different way as done on HLF v0.6, the performance evaluation on HLF v1.0 or higher has been done by considering the HLF parameters, which were added and controllable since HLF v1.0. With varying their values, the throughput and latency are explored in literature [18] and [19]. Especially, the scalability is additionally considered when the number of network participants increases in [18]. Simple optimizations for improving the overall system performance are discussed in [19]. Besides, the impacts of system components in HLF on the performance are investigated, such as number of endorsing peers [20], chaincode types [21], HLF database types [22], and delayed block propagation from an ordering service [23].

However, the performance evaluation studies aforementioned in this subsection have the limitation that it is still impossible to predict the performance of an HLF network for a given network setup. In other words, they may be able to help to understand performance trends of HLF, but cannot be used to estimate the latency of an established HLF network.

B. HLF Performance Modeling

HLF performance modeling work is to provide or design a performance model of HLF v0.6 [24] or HLF v1.0 or higher [25]–[28]. A stochastic reward net (SRN) model of PBFT is proposed for a PBFT-based HLF network in [24]. Note that PBFT is available for HLF v0.6 only as described earlier. For HLF v1.0 or higher, a performance model of HLF with Kafka/ZooKeeper, which is a new consensus algorithm released in HLF v1.0, is proposed using several methods, such as SRN [25], generalized stochastic petri nets (GSPNs) [26], a hierarchical model based on transaction execution and validation [27], and a theoretical latency model [28].

However, the performance modeling studies aforementioned are either based on HLF v0.6 [24] or fail to show the probability distribution of HLF latency [25]–[28]. Specifically, the mean HLF latency were provided from measurements in the previous studies including [25]–[28], but they do not reveal the distribution of the HLF latency, which is generally more necessary for a reliable design of HLF-based IoT networks.

III. HYPERLEDGER FABRIC OVERVIEW

HLF is a private blockchain platform for a modular architecture, which is one of the sub-projects in the Hyperledger Project [29]. In the other blockchain platforms, a deterministic programming language is compulsory to prohibit ledgers from diverging, such as Solidity in Ethereum. In contrast, the novel structure of HLF v1.0 or higher not only enables several business logics to be written in general-purpose programming languages, but also prevents ledger bifurcation at the same time [30]. In this section, we first provide the definitions of some important system components and parameters in HLF, then demonstrate the transaction flow consisting of three phases. Note that we refer to the Hyperledger official website [29] and Read the Docs [31] for accuracy. The overall structure of HLF can be also found in Fig. 1.

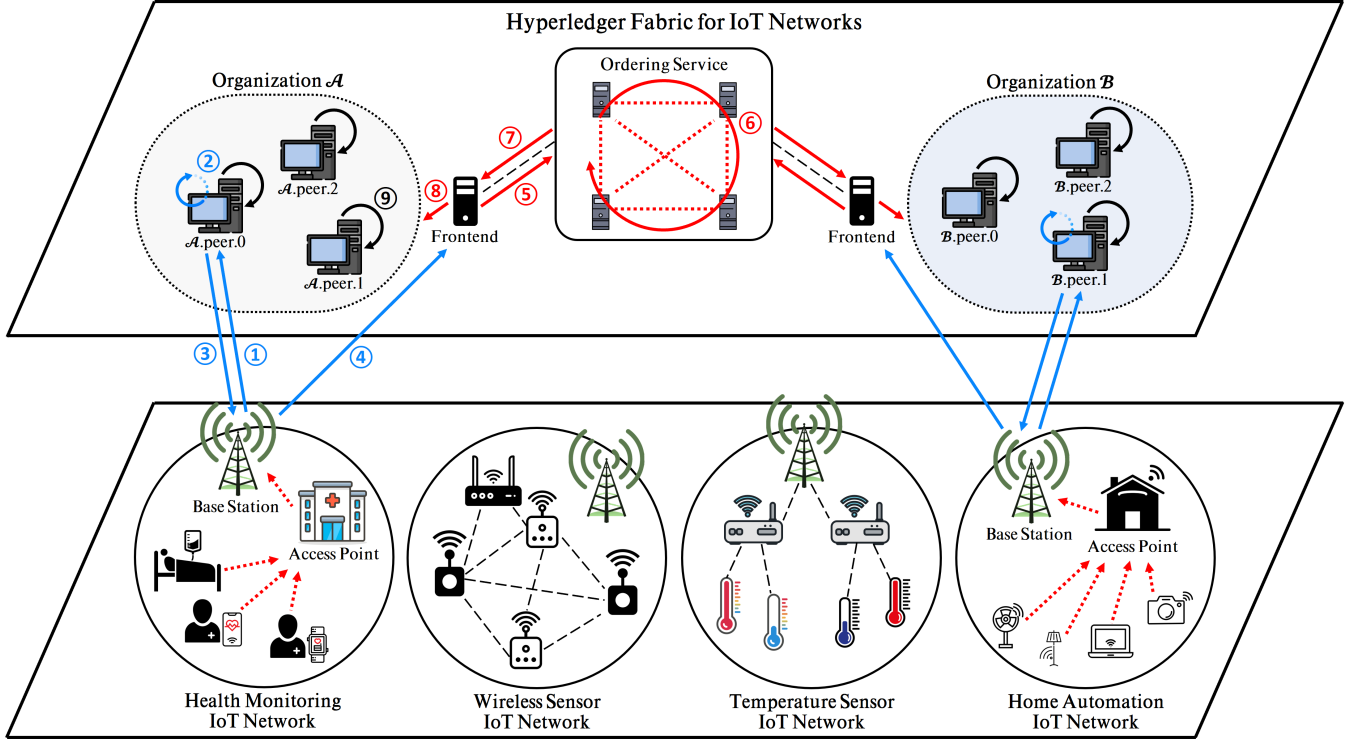


Fig. 1: Structure of HLF-enabled IoT networks.

A. System Components

1) *Peer*: The peer refers to a node which serves as a legitimate member in an HLF network. The peer is mainly classified under three types: committing peer (i.e., committer), endorsing peer (i.e., endorser), and ordering peer (i.e., orderer).

- The committing peer refers to a normal peer allowed to maintain a copied ledger and to validate newly delivered blocks. Note that the committing peer is not empowered to simulate transaction proposals or to generate new blocks.
- The endorsing peer refers to a particular committing peer entitled to simulate a transaction proposal from a client and to return the obtained result. In order to execute the proposal, the endorsing peer is allowed to access chaincodes, in which business logics and functions are defined.
- The ordering peer refers to a special node in an ordering service. Note that the ordering service is a node cluster to generate new blocks. Unlike the other peers, the minimum number of required ordering peers are determined according to the method for implementing the ordering service. For example, it is necessary for a Kafka/ZooKeeper-based ordering service to have at least four ordering nodes (i.e., Kafka nodes) for crash fault tolerance (CFT).

2) *Ledger*: The ledger is composed of a blockchain storage and the state database. The blockchain storage includes all transactions, which have been generated until the present, in the form of an immutable chain of multiple blocks. The state database contains the current values of key-value pairs, which have been modified and created by clients [31]. In other words,

the blockchain storage is the history of generated transactions for data updates in the state database, and the state database is a key-value database to hold existing keys and their latest data.

3) *Organization*: The organization refers to a group, which peers appertain to. In order to serve as a valid member in HLF, a peer has to possess a credential issued by the organization that it wants to join. Thus, the organization is required to enroll a membership service provider, which is an abstract component to generate credentials, to participate in an HLF network [31].

4) *Ordering Service*: The ordering service is a node cluster composed of several ordering nodes, which are eligible for manufacturing new blocks and for performing a deployed consensus protocol on every new block. The ordering service can be implemented with one of the following implementation methods: solo, Kafka/ZooKeeper, Raft [32], and Byzantine fault tolerant state machine replication (BFT-SMaRt) [33]. Note that the BFT-SMaRt-based ordering service is not officially released.

The Kafka/ZooKeeper-based ordering service has been currently the most widely used since it was available in HLF v1.0. This ordering service is based on two off-the-shelf software programs: Apache Kafka and Apache ZooKeeper. Apache Kafka is a distributed message management software platform ensuring CFT [34]. Apache ZooKeeper is employed to assist Apache Kafka in configuration data management and distributed synchronization [35]. We decide to deploy the Kafka/ZooKeeper-based ordering service in our HLF system.

5) *Channel*: The channel is a sub-network in which a set of peers manages a channel-specific ledger. In other words,

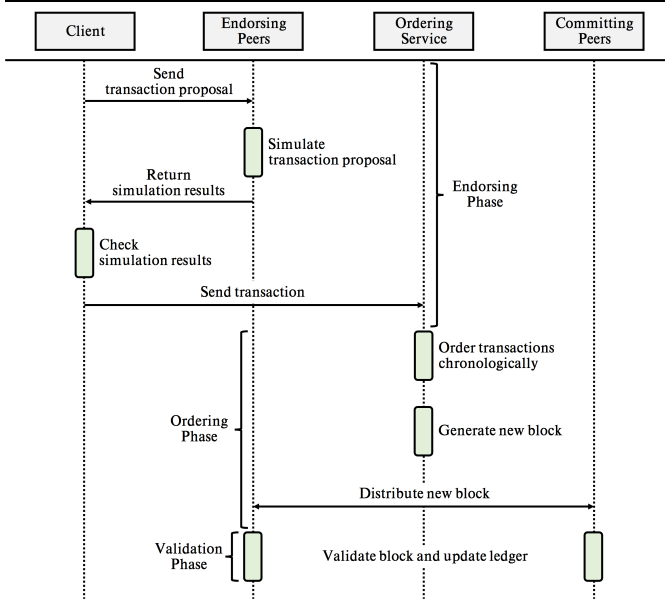


Fig. 2: Transaction flow in HLF.

each channel is allowed to possess its own ledger for data confidentiality, which is shared among the participating peers only. Therefore, the ledger in a channel can prevent itself from being tampered by unauthorized peers. In this paper, we use the term *HLF channel* for this channel component in order to avoid confusion with communication channel.

6) *Chaincode*: The chaincode (i.e., smart contract) is a program, which defines business logics and functions to append new data or update retained data in the ledger. For example, a client can specify a business logic in a transaction proposal, and transmit it to the endorsing peers for data update. In general, the chaincode is isolated for data integrity to protect itself against security threats, such as modification attacks.

7) *Block Size*: The block size is one of the configurable parameters of the ordering service. This parameter defines the maximum number of transactions in one block. In other words, the block size determines how many transactions the ordering service can collect the most in one block. The transactions are promptly exported from the ordering service as a new block, when the number of transactions in the waiting queue reaches the pre-defined block size value.

8) *Block-generation Timeout*: The block-generation timeout is another configurable parameter of the ordering service. This parameter defines the maximum time to wait for other transactions to be exported as a new block since the first transaction arrived at the waiting queue. When the first transaction arrives at the empty waiting queue in the ordering service, a timer is simultaneously set to the pre-defined block-generation timeout value. Once the timer expires, the ordering service exports the pending transactions in the form of a block, no matter how few transactions have accumulated in the waiting queue. In other words, the block-generation timeout is to prevent transactions from spending a long time in the ordering service. It is especially effective if the pre-defined block size is fairly large or if new transactions are not frequently generated.

B. Transaction Flow

Figure 2 illustrates the transaction flow in HLF. Transactions in HLF are appended to the ledger through three phases: endorsing phase, ordering phase, and validation phase. The processing phases enable HLF networks not only to support general-purpose programming languages, but also to remain tamper-proof. In this subsection, we describe the transaction flow in HLF for data updates.

1) *Endorsing Phase*: The endorsing phase is started with the transaction proposal generation at the client. The main objective of this phase is to collect the sufficient number of simulation results of the proposal (i.e., endorsement), according to the endorsement policy. Hence, the endorsing peers are asked to execute the proposal against their own copied ledgers, and return the results to the client. Note that the endorsement policy specifies by which endorsing peers the transaction has to be endorsed [36].

The endorsement includes the signature of the signing endorsing peer and a read/write set. The read set includes the key to update and its latest version, which already has been committed to the ledger previously. The write set includes the key to update and its new value, with which the client hopes to update the value of the key. The client investigates whether all the delivered endorsements have exactly the same simulation results from one another. If they are identical, the client transmits them to the ordering service as a transaction. Otherwise, they are discarded.

2) *Ordering Phase*: The ordering phase is the second phase in which every delivered transaction is ordered chronologically and included in a new block. The ordering service accumulates transactions in each HLF channel, and then generates a new block. The new block is transmitted to peers for the validation phase in the corresponding HLF channel through the gossip protocol. Note that we focus on the Kafka/ZooKeeper-based ordering service, which is currently the most widely used and commonly discovered in literature listed in Section II.

3) *Validation Phase*: The validation phase is the last phase in which the new block is validated by each peer individually. In this phase, a peer, which has successfully received the block, mainly conducts two sequential verifications: (1) validation system chaincode (VSCC) verification and (2) multi-version concurrency control (MVCC) verification. The VSCC verification is to make sure that a transaction has been endorsed by proper endorsing peers against the endorsement policy. If the transaction has sufficient endorsements, it is marked as valid [30]. Otherwise, it is prohibited from updating the ledger and marked as invalid.

On the other hand, the MVCC verification is to investigate if the key versions captured during the endorsing phase still remain the same as those in the current ledger locally owned by the peer [30]. If they are the same as each other, the transaction is allowed to update the ledger with the data, and the key version is changed. In contrast, the transaction is considered as invalid if any of the previously conveyed transactions have already updated the identical data (i.e., the one with the same key-value) ahead of it. The key-version of data changes each time the data is successfully updated [36].

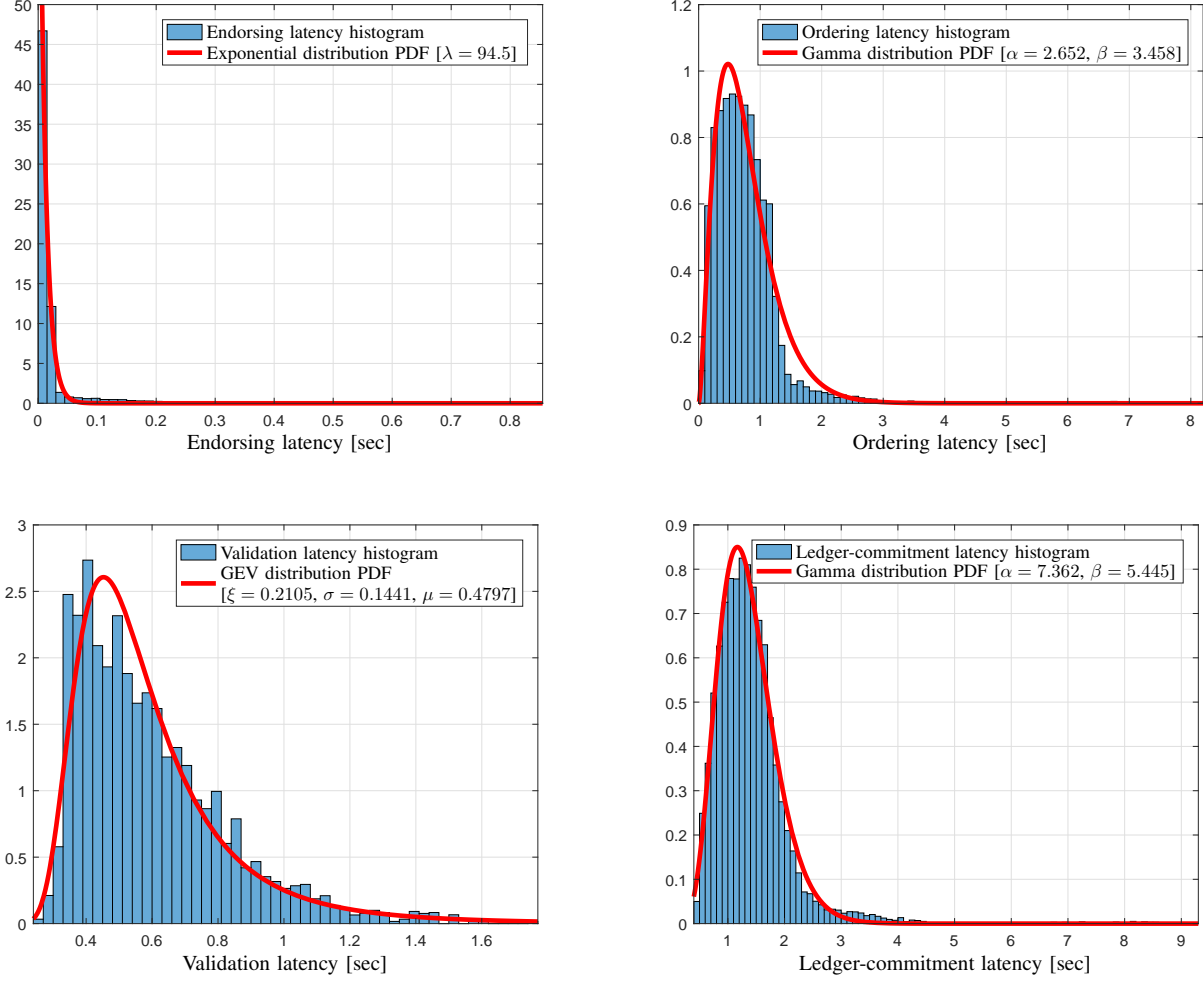


Fig. 3: Histograms of the endorsing latency, ordering latency, validation latency, and ledger-commitment latency, where $S_b = 10$, $T_b = 1$ [sec], and $\lambda_t = 10$ transactions/second.

C. HLF-enabled IoT Networks

Figure 1 demonstrates an HLF-enabled IoT network preserving data generated from IoT devices. A group of IoT devices can establish an IoT network, while HLF facilitates such IoT networks to exploit the blockchain storage for IoT data management. For example, the access points (APs) receive data generated by IoT devices in the health monitoring and home automation networks, as shown in Fig. 1. In the health monitoring network, IoT devices deliver new data about patient condition to the AP for periodic monitoring. The AP then forwards the delivered IoT data to the HLF network.

The proposal including the data sent from the IoT device is transmitted to endorsing peers, and the endorsing peers simulate the data against its own ledger using the smart contract. Upon completion of the execution process, the endorsing peer returns the result with its signature to the IoT device. Note that if the endorsement policy requires multiple endorsing peers, the IoT device has to make sure that all returned results are identical to each other. After the IoT device delivers the endorsement as a transaction to the ordering

service, the ordering service generates a new block. The new block including the transaction is conveyed to peers for the validation phase, and then the transaction is finally allowed to update the ledger if it is successfully validated.

IV. HLF LATENCY MODELING

In this section, we conduct HLF latency modeling based on the probability distribution fitting method. We first define latency types in HLF, and provide the experimental setup of our HLF network, used for experiments. For the probability distribution fitting method, we define three useful probability distributions with their probability density functions (PDFs) and cumulative distribution functions (CDFs), and finally provide our HLF latency model. For evaluating goodness-of-fit of our modeling, we also conduct the Kolmogorov-Smirnov (KS) test. The feasibility conditions for our latency modeling are also discussed with providing the cases, for which the probability distribution fitting method does not work well.

A. Latency Types in HLF

Before modeling the HLF latency, we first divide the total elapsed time of the data in the HLF network according to the transaction-processing stages, described in Section III-B, such as the endorsing latency, the ordering latency, the validation latency, and the ledger-commitment latency (i.e., the total latency). Note that we exclude the communication latency spent from an IoT device to reach the HLF network, as it is more depending on the communication standard that IoT devices use and it has already been explored in much literature.

1) *Endorsing Latency*: The endorsing latency refers to the time taken to request endorsing peers to endorse a transaction, and to receive their responses. To be specific, it is defined as the sum of the latencies for step 1, 2, 3, and 4 in Fig. 1.

2) *Ordering Latency*: The ordering latency refers to the time taken to await until the transaction is exported as a new block from the ordering service. It is defined as the sum of the latencies for step 5, 6, 7, and 8 in Fig. 1. Note that the latency for step 6 consists of the consensus time and the waiting time for other transactions to be released as part of a new block. In contrast, the latency for step 8 is the sum of transmission time and the waiting time of the released block for the validation phase. Thus, it may be considered as part of the validation latency. In this paper, however, we include this latency into the ordering latency, when we depict the histograms in Figs. 3 and 6. Note that the latency for step 8 may be highly likely to work as a bottleneck if the previous block requires long time to be validated.

3) *Validation Latency*: The validation latency refers to the time taken to validate and commit the block with ledger update. This latency is defined as the latency for step 9 in Fig. 1. All transactions in the same block are sequentially validated, but committed to the ledger all together as a batch. Therefore, they have the identical validation latency from each other. Note that the validation latency may vary according to peers. In this paper, this latency is measured at the endorsing peer.

4) *Ledger-commitment Latency (Total Latency)*: The ledger-commitment latency refers to the time taken to completely process a transaction from the beginning. Thus, it is the sum of the endorsing, ordering, and validation latencies.

B. Experimental Setup

For the implementation of our HLF network, we exploit the HLF v1.3 sample network released at [31] on one physical machine. The machine running the HLF network is with Intel® Xeon W-2155 @ 3.30 GHz processor and 16 GB RAM. In addition, we newly bring up a Kafka/ZooKeeper-based ordering service consisting of four Kafka nodes, three ZooKeeper nodes, and three frontend nodes that are connected to the Kafka node cluster in the network. Note that the frontend node is not only to inject transactions from clients into the Kafka node cluster, but also to receive new blocks, which will be disseminated to peers. The HLF network has one endorsing peer and two committing peers. Note that the number of committing peers may not affect the ledger-commitment latency because they can only validate newly delivered blocks and hold copied ledgers [37].

TABLE I: Estimated Gamma distribution parameters (α, β), the KS test results, the average latency of empirical results \bar{T}_{ep} , and the average latency of the best-fit distribution \bar{T}_{bf} for the ledger-commitment latency.

	λ_t	Estimated (α, β)	KS Statistics	Empirical Avg. \bar{T}_{ep}	Best-fit Avg. \bar{T}_{bf}
$S_b = 20$ $T_b = 1$	10	(8.9573, 5.5858)	0.0457	1.6066	1.6035
	11	(9.5112, 6.0407)	0.0466	1.5767	1.5745
	12	(9.3159, 6.2078)	0.0503	1.4969	1.5006
	13	(10.0333, 6.2937)	0.049	1.5891	1.5941
$S_b = 25$ $T_b = 1$	17	(9.7902, 6.0267)	0.0504	1.6141	1.6244
	18	(9.1368, 6.131)	0.0595	1.4908	1.4902
	19	(9.005, 5.9462)	0.0564	1.5098	1.5144
	20	(8.2069, 5.395)	0.051	1.5232	1.5212
$S_b = 10$ $T_b = 2$	8	(7.181, 4.0151)	0.0388	1.8289	1.7884
	9	(6.8603, 4.6625)	0.0437	1.4658	1.4713
	10	(5.6829, 4.355)	0.0457	1.3517	1.3049
	11	(7.1636, 4.1801)	0.0444	1.7513	1.7137
$S_b = 20$ $T_b = 2$	15	(7.6898, 4.6474)	0.0358	1.6587	1.6566
	16	(8.4486, 5.1794)	0.0474	1.6406	1.6311
	17	(8.0874, 5.2866)	0.0419	1.5323	1.5297
	18	(8.3269, 4.8638)	0.0404	1.7437	1.712
$S_b = 20$ $T_b = 3$	15	(7.9739, 4.9723)	0.0382	1.616	1.6036
	16	(7.608, 4.9499)	0.0394	1.5351	1.537
	17	(7.0015, 4.9697)	0.0403	1.3992	1.4088
	18	(5.7078, 4.1482)	0.0513	1.3902	1.3759
$S_b = 30$ $T_b = 3$	23	(8.0788, 4.6915)	0.0369	1.727	1.722
	24	(7.0546, 4.527)	0.0395	1.5652	1.5583
	25	(6.3698, 4.4257)	0.0468	1.4345	1.4392
	26	(7.3836, 4.8698)	0.0435	1.5125	1.5162

Each test run includes 1,000 transaction proposals to submit. All proposals attempt to update a key-value set, using appropriate arguments for the *changeCarOwner* function defined in the *Fabcar* chaincode in [31]. Each of the equipped frontend nodes has an equal probability of being selected to relay a transaction from our client to the Kafka node cluster, and to make a new block propagated. Note that the generated proposals in one test run do not access the same key-value set. Hence, we do not consider the MVCC violation in this paper.

The client generates new transactions at the rate of λ_t transactions/sec, and their inter-generation times follow an exponential distribution. At each iteration of test runs, we not only vary the transaction generation rate λ_t , but also measure the endorsing, ordering, validation, and ledger-commitment latency in order to analyze the impact of increasing λ_t . Note that S_b and T_b refer to the block size and block-generation timeout, respectively.

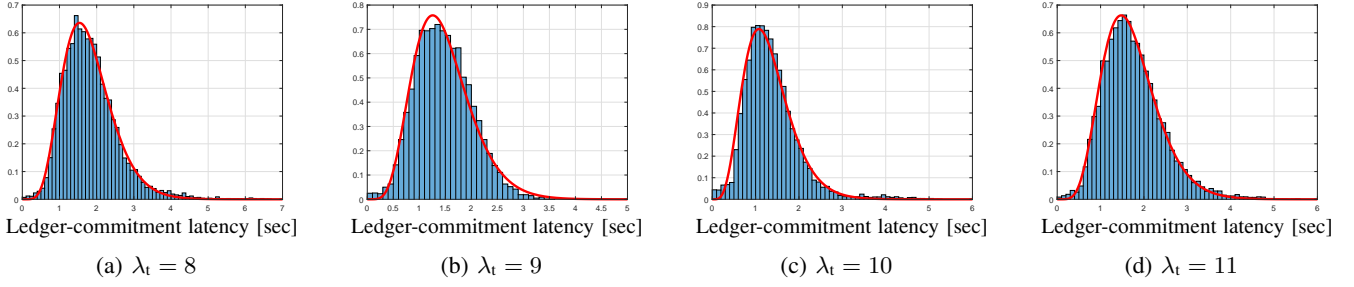


Fig. 4: Histograms and their best-fit Gamma distributions of the ledger-commitment latency for different values of the transaction generation rates λ_t , where $S_b = 10$ and $T_b = 2$ [sec].

C. Useful Probability Distributions

In this subsection, we provide the definitions of some probability distributions, which are used for our latency modeling.

1) *Exponential Distribution*: The exponential distribution is the probability distribution of time intervals in a Poisson process. This distribution has the PDF and the CDF, respectively, as

$$f(x) = \lambda e^{-\lambda x}, \quad F(x) = 1 - e^{-\lambda x} \quad (1)$$

where λ is the rate parameter for $\lambda > 0$.

2) *Gamma Distribution*: The Gamma distribution is a two parameter frequency distribution [38]. For $\alpha > 0$ and $\beta > 0$, the PDF and the CDF of the Gamma distribution are respectively defined as

$$f(x) = \frac{\beta^\alpha}{\Gamma(\alpha)} x^{\alpha-1} e^{-\beta x}, \quad F(x) = \frac{1}{\Gamma(\alpha)} \gamma(\alpha, \beta x) \quad (2)$$

where $\Gamma(\alpha)$ is the gamma function, defined as $\Gamma(\alpha) = \int_0^\infty x^{\alpha-1} e^{-x} dx$, and $\gamma(\alpha, x)$ is the lower incomplete gamma function, defined as $\gamma(\alpha, x) = \int_0^x t^{\alpha-1} e^{-t} dt$ for $x \geq 0$ [39]. Note that α is the shape parameter, and β is the inverse scale parameter (i.e., the rate parameter).

3) *Generalized Extreme Value (GEV) Distribution*: The GEV distribution encompasses the three standard extreme value distributions: Gumbel ($\xi = 0$), Fréchet ($\xi > 0$), and Weibull ($\xi < 0$) [40]. Depending on the shape parameter, denoted as ξ , the GEV distribution results in one of the three probability distributions, which are also respectively referred to as GEV distribution's Type I, II, and III in the listed order above. The PDF and the CDF of the GEV distribution are respectively given as the following expressions for $-\infty < x \leq \mu - \frac{\sigma}{\xi}$ when $\xi < 0$, for $\mu - \frac{\sigma}{\xi} \leq x < \infty$ when $\xi > 0$, and for $-\infty \leq x \leq \infty$ when $\xi = 0$ [41]

$$f(x) = \begin{cases} \frac{\{1 + \xi (\frac{x-\mu}{\sigma})\}^{-[(\frac{1}{\xi})-1]}}{\sigma \exp\left\{\left(1 + \xi (\frac{x-\mu}{\sigma})\right)^{-\frac{1}{\xi}}\right\}}, & \text{if } \xi \neq 0 \\ \frac{1}{\sigma} \exp\left\{-\frac{x-\mu}{\sigma} - \exp\left[-\frac{x-\mu}{\sigma}\right]\right\}, & \text{if } \xi = 0 \end{cases} \quad (3)$$

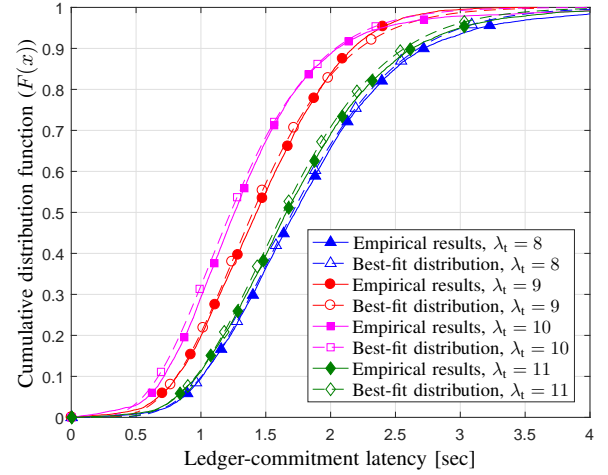


Fig. 5: Empirical CDFs and the best-fit Gamma distribution CDFs of the ledger-commitment latency for different values of the transaction generation rates λ_t , where $S_b = 10$ and $T_b = 2$ [sec].

$$F(x) = \begin{cases} \exp\left\{-\left(1 + \xi \left(\frac{x-\mu}{\sigma}\right)\right)^{-\frac{1}{\xi}}\right\}, & \text{if } \xi \neq 0 \\ \exp\left\{-\exp\left\{-\frac{x-\mu}{\sigma}\right\}\right\}, & \text{if } \xi = 0 \end{cases} \quad (4)$$

Note that μ is the location parameter, and σ is the scale parameter.

D. Latency Modeling and Validation

1) *Latency Modeling*: For the latency modeling, we first capture at least over 20,000 transaction samples and obtain the histogram for each latency type defined in Section IV-A. We then seek out the best-fit probability distribution for each latency histogram. The discovered best-fit distributions are as follows.

- Endorsing latency – Exponential distribution
- Ordering latency – Gamma distribution
- Validation latency – GEV distribution
- Ledger-commitment latency – Gamma distribution

Once the best-fit distributions are determined, we estimate the distribution parameters, such as λ for the exponential

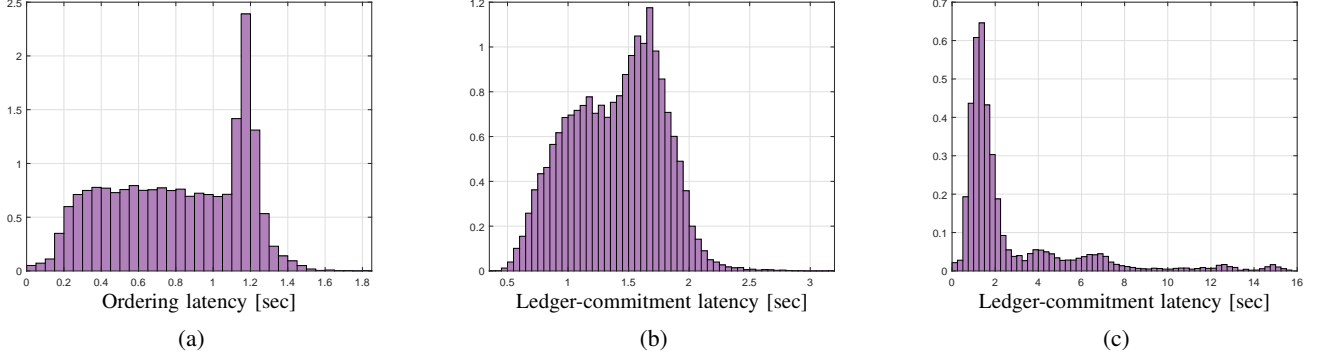


Fig. 6: Ordering latency and ledger-commitment latency histograms of infeasible latency modeling cases.

distribution, (μ, σ, ξ) for the GEV distribution, and (α, β) for the Gamma distribution, using the curve fitting tool such as the nonlinear regression method in Matlab.¹ The histogram and discovered best-fit distribution with estimated parameter for each latency type are provided in Fig. 3. From Fig. 3, we can see that the discovered best-fit distributions match well with the histograms, especially with the ledger-commitment latency.

For the ledger-commitment latency, we also provide the histograms and the PDFs of their best-fit Gamma distributions in Fig. 4, and the CDFs of the empirically measured values and their best-fit Gamma distributions in Fig. 5. The estimated Gamma distribution parameter pairs of the ledger-commitment latency for various HLF environments are also provided in Table I. Note that \bar{T}_l refers to the average ledger-commitment latency for a given HLF environment. In Table I, empirically obtained \bar{T}_l is denoted as \bar{T}_{ep} , and \bar{T}_l from the best-fit distribution is denoted as \bar{T}_{bf} .

From Figs. 4 and 5, we can see that not only the PDFs but also the CDFs of the best-fit Gamma distribution matches well with the empirically obtained ones. From Fig. 4 and \bar{T}_l , for $T_b = 2$ [sec] and $S_b = 10$ in Table I, we can see that \bar{T}_l decreases as λ_t increases since it makes new blocks generated faster in the ordering service. However, \bar{T}_l increases when λ_t becomes 11. This is because there is large load at the validation phase as the block-generation rate becomes higher. Hence, some blocks start to wait for the validation process, which increases \bar{T}_l .

2) *Modeling Validation*: In order to validate and improve the reliability of our latency model, we include KS test results in Table I. The KS test is a statistical test to evaluate goodness-of-fit [42]. It compares a set of data with a given probability distribution, then decides if the data set is consistent with the given distribution [43]. The decision is made based on the maximum difference between the empirical CDF of the data set and the hypothetical CDF (i.e., the CDF of the given distribution) [43].

The estimated parameters and KS statistics are averaged over ten test runs at 0.01 significance level. The critical value is computed as 0.0513. In other words, the latency model can be considered as reliable if the KS statistics value of a data

set is less than 0.0513. As an example, Fig. 4 and 5 show the ledger-commitment latency, when $S_b = 10$ and $T_b = 2$ [sec] for $\lambda_t = 8, 9, 10$ and 11. In Table I, all cases in those figures have smaller KS statistics values (i.e., 0.0388, 0.0437, 0.0457, and 0.0444, respectively) than the critical value. Thus, the test is passed for all cases. However, in Table I, when $S_b = 25$ and $T_b = 1$ for $\lambda_t = 18$ and 19, their KS statistics values are slightly larger than the critical value, but even in those cases, we can see that they still have the similar mean latency \bar{T}_{bf} to each of their \bar{T}_{ep} .

E. Feasibility Conditions for Latency Modeling

During the modeling process, it is found that there exist some cases in which histograms of \bar{T}_l do not fit well into a known probability distribution. In other words, the probability distribution fitting method is not always applicable. We have discovered two environments that make the probability distribution fitting method infeasible as follows.

1) Timeout-dominant Block Generation Environment:

When the transaction generation rate λ_t is small, while the block-generation timeout value T_b is relatively large, few of transactions (or even one transaction) may stay in the waiting room for the ordering service in the ordering phase most of their time, and become a block once the timeout expires. In this case, a large portion of transactions can have the ordering latency equal to T_b . As an example of such case, the histograms of the ordering latency and the ledger-commitment latency are shown in Figs. 6a and 6b, respectively, where $S_b = 10$, $T_b = 1$ [sec], and $\lambda_t = 3$. As shown in Fig. 6a, there is a peak when the ordering latency is 1.2 seconds, and in this case, the percentage of blocks, which are exported from the ordering service by the block-generation timeout expiration, is 99.8%. Due to this, as shown in Fig. 6b, the ledger-commitment latency has the distribution, which is difficult to define using any known probability distributions.

2) Block Size-dominant Block Generation Environment:

When the block size S_b is small, while the transaction generation rate λ_t is large, most blocks are filled with transactions up to S_b quickly, so blocks are generated fast with the full size from the ordering service. In this case, even though the ordering latency is small, there can be large load at the validation phase due to the fast block generation, which

¹For better fitting results, we exclude some test runs with remarkably long mean latency similar to conventional fitting work such as [24].

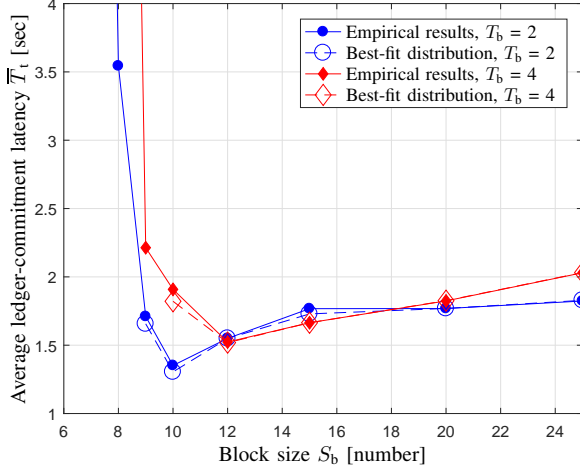


Fig. 7: Effect of the block size on the ledger-commitment latency, where $\lambda_t = 10$ and $T_b = 2$ and 4 [sec].

TABLE II: Estimated Gamma distribution parameters (α, β), the KS test results, the average latency of empirical results \bar{T}_{ep} , and the average latency of the best-fit distribution \bar{T}_{bf} for the ledger-commitment latency for $\lambda_t = 10$.

S_b	T_b	Estimated (α, β)	KS Statistics	Empirical Avg. \bar{T}_{ep}	Best-fit Avg. \bar{T}_{bf}
9	2	(8.9573, 5.5858)	0.0457	1.6066	1.6035
10		(9.5112, 6.0407)	0.0466	1.5767	1.5745
12		(9.3159, 6.2078)	0.0503	1.4969	1.5006
15		(10.0333, 6.2937)	0.049	1.5891	1.5941
10	1.75	(9.7902, 6.0267)	0.0504	1.6141	1.6244
	2.00	(9.1368, 6.131)	0.0595	1.4908	1.4902
	2.25	(9.005, 5.9462)	0.0564	1.5098	1.5144
	2.50	(8.2069, 5.395)	0.051	1.5232	1.5212

makes blocks wait for validation. Hence, there can be many transactions with long waiting time to enter the validation phase. As an example of such case, the histogram of the ledger-commitment latency is provided in Fig. 6c, where $S_b = 15$, $T_b = 0.75$ [sec], and $\lambda_t = 10$. As shown in this figure, there are long-tail outliers more frequently in the distribution (e.g., the cases with the ledger-commitment latency longer than 4 seconds), which makes it difficult to fit to a known probability distribution.

Note that the two environments, discussed above, are the cases where S_b or T_b is too small or large, so a large portion of transactions experience long latency in the ordering or validation phase. For delay-sensitive applications or services, such HLF parameter setups will be generally avoided.

V. INFLUENTIAL PARAMETER ANALYSIS ON LATENCY

From the viewpoint of an IoT application, which handles time-sensitive jobs [12] and desires faster transaction commitment, it is important to design HLF in the way to minimize the ledger-commitment latency. As defined in Section III-A,

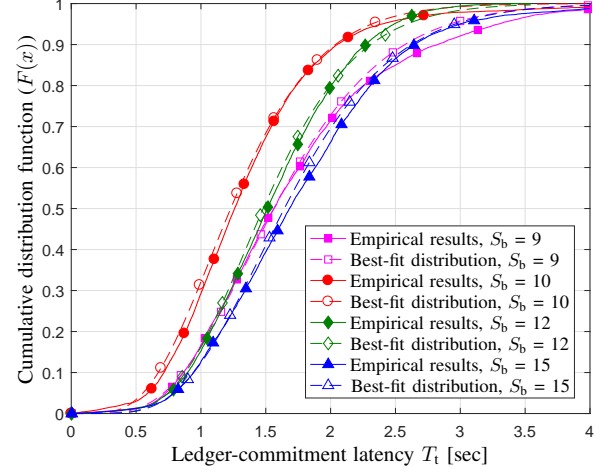


Fig. 8: Empirical CDFs and best-fit distribution CDFs of the ledger-commitment latency, where $\lambda_t = 10$ and $T_b = 2$ [sec].

the block size and block-generation timeout parameters are important to control how fast new blocks are produced from the ordering service, i.e., the block-generation rate. In addition, we can see in Table I that the transaction generation rate also affects the ledger-commitment latency. Focusing on the three parameters, therefore, we explore their impacts on the ledger-commitment latency. Moreover, we discuss how to optimally determine the transaction generation rate, block size, and block-generation timeout parameters to minimize the ledger-commitment latency.

A. Impact of Transaction Generation Rate

Table I demonstrates the impact of the transaction generation rate λ_t for different S_b and T_b on the average ledger-commitment latency \bar{T}_t for both empirical and best-fit distribution results. From Table I, we can observe two conflicting effects of the transaction generation rate on the ledger-commitment latency. Higher λ_t makes transactions exported from the ordering service faster, leading to an increase in the block-generation rate at the ordering service. Due to this, the lowest \bar{T}_t can be achieved by increasing λ_t . For instance, when S_b is 20 and T_b is 1 [sec] in Table I, \bar{T}_{ep} decreases from 1.6066 to 1.4969 as λ_t increases from 10 to 12 transactions/second.

However, \bar{T}_t does not continuously decrease, and starts to increase after some point of λ_t . As seen in Table I, when S_b is 20 and T_b is 1 [sec], \bar{T}_{ep} increases from 1.4969 to 1.5891 as λ_t increases from 12 to 13 transactions/second. This is because the block validation rate does not increase despite faster block-generation. New blocks need to wait for the validation. From these observations, we can see that the optimal λ_t , which minimizes \bar{T}_t , exists for a given HLF setup.

B. Impact of Block Size

Figures 7 and 8 illustrate the impact of the block size S_b on \bar{T}_t and the CDFs of the ledger-commitment latency, respectively, for empirical results and the best-fit distributions.

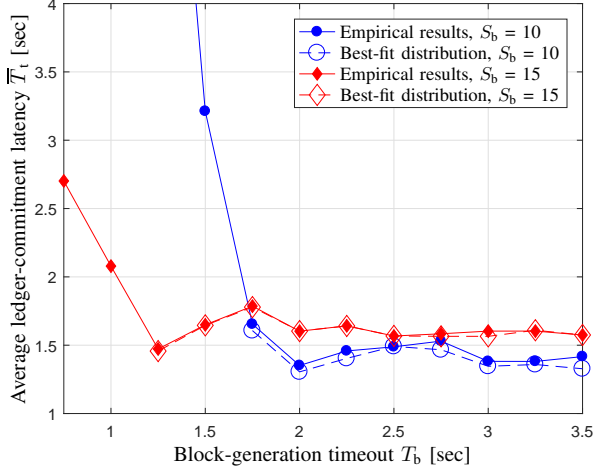


Fig. 9: Effect of the block-generation timeout on the ledger-commitment latency, where $\lambda_t = 10$ and $S_b = 10$ and 15.

Note that the probability distribution fitting results with KS statistics values are provided in Table II (see the values for $S_b = 9, 10, 12$, and 15 and $T_b = 2$ [sec]). From Figs. 7 and 8, we can see that both the average and the CDFs of the ledger-commitment latency of the best-fit distributions are well-matched with those of the empirical results.

From Fig. 7, we can also see that when the block size S_b is small (e.g., $S_b < 8$), the average ledger-commitment latency \bar{T}_t is extremely high. This is because the peers receiving blocks cannot promptly start to validate them since blocks are generated too fast due to the small block size. Therefore, new blocks gradually stack up in each peer's queue for the validation, which leads to long validation delay. As S_b increases, \bar{T}_t decreases because the block-generation rate decreases and the waiting time at the validation phase becomes lower as well. However, when S_b increases beyond certain values (e.g., $S_b > 10$ for $T_b = 2$ [sec] and $S_b > 12$ for $T_b = 4$ [sec]), \bar{T}_t increases again. In this case, the validation latency is no longer long, but transactions need to wait longer for others to be included into a block in the ordering phase due to the large size of S_b . As S_b keeps increasing, \bar{T}_t could eventually saturate as most of the new blocks are generated by the timeout expiration before they are generated by fully collected S_b transactions.

C. Impact of Block-generation Timeout

Figures 9 and 10 demonstrate the impact of the block-generation timeout T_b on \bar{T}_t and the CDFs of the ledger-commitment latency, respectively, for empirical results and the best-fit distributions. Note that the probability distribution fitting results with KS statistics values are provided in Table II (see the values for $S_b = 10$ and $T_b = 1.75, 2.00, 2.25$, and 2.50 [sec]). From Figs 9 and 10, we can see that both the average and the CDFs of the ledger-commitment latency of the best-fit distributions are well-matched with those of the empirical results.

From Fig. 7, we can also see that when the block-generation timeout T_b is short (e.g., $T_b < 1.5$ [sec] for $S_b = 10$ and

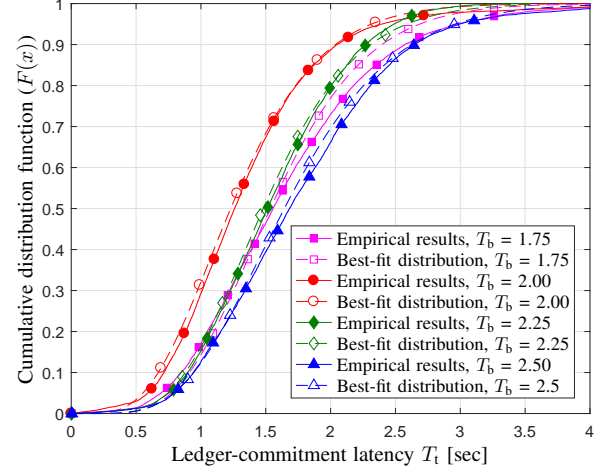


Fig. 10: Empirical CDFs and best-fit distribution CDFs of the ledger-commitment latency, where $\lambda_t = 10$ and $S_b = 10$.

$T_b < 0.5$ [sec] for $S_b = 15$), the average ledger-commitment latency \bar{T}_t is extremely high for the same reason as explained in Section V-B due to the short block-generation timeout. As T_b increases, \bar{T}_t decreases and the waiting time at the validation phase also becomes lower. However, when T_b increases beyond certain values (e.g., $T_b < 2$ [sec] for $S_b = 10$ and $T_b < 1.25$ [sec] for $S_b = 15$), \bar{T}_t increases again. In this case, the validation latency is no longer long, but transactions need to wait longer for others to be included into a block in the ordering phase due to the long T_b . As T_b keeps increasing, \bar{T}_t could eventually saturate as most of the new blocks are generated because S_b transactions are collected before the timeout expires.

Besides, we found that \bar{T}_t can be more sensitively changed according to λ_t for longer T_b . Specifically, in Table I, for $S_b = 20$, when T_b is 2 [sec], \bar{T}_{ep} is 1.6587 and 1.7437, respectively, for $\lambda_t = 15$ and 18. However, when T_b becomes 3 [sec], \bar{T}_{ep} is 1.616 and 1.3902, respectively, for $\lambda_t = 15$ and 18. The difference of \bar{T}_{ep} is larger for $T_b = 3$ [sec] (i.e., 0.2258) than that for $T_b = 2$ [sec] (i.e., 0.085).

VI. CONCLUSIONS

This paper provides the latency model for HLF-based IoT networks, where latency-critical tasks are generally handled. From the histograms of the ledger-commitment latency obtained from experiments in HLF, we figure out that the ledger-commitment latency can be modeled as a Gamma distribution in various HLF setups. We then conduct the KS test and prove that our modeling is reliable. Moreover, we explore the impacts of three important HLF parameters (i.e., transaction generation rate, block size, and block-generation timeout) on the ledger-commitment latency. Specifically, when they are set to be small, the ledger-commitment latency is fairly high due to the fast block generation that causes long validation latency. Hence, the ledger-commitment latency decreases as those values increase, but eventually it increases again since the latency in the ordering phase increases. From this observation,

it is shown that the proper setup of HLF parameters are important to lower the ledger-commitment latency. This can be done more easily using our latency modeling results as the implementation and experiments of HLF can be omitted. Finally, this paper can serve as a guideline not only to predict the mean and the distribution of the ledger-commitment latency, but also to optimally construct HLF-enabled IoT networks with low latency.

REFERENCES

- [1] S. Nakamoto, "Bitcoin: A peer-to-peer electronic cash system," 2008. [Online]. Available: <https://bitcoin.org/bitcoin.pdf>.
- [2] M. Mittala, R. Sangania, and K. Srivastava, "Testing data integrity in distributed systems," in *Proc. Int. Conf. Adv. Comput. Technol. Appl. (ICACTA)*, Mumbai, India, Mar. 2015, pp. 1–7.
- [3] A. Narayanan, J. Bonneau, E. Felten, A. Miller, and S. Goldfeder, *Bitcoin and Cryptocurrency Technologies: A Comprehensive Introduction*. Princeton, NJ, USA: Princeton University Press, 2016.
- [4] A. Yazdinejad, R. M. Parizi, A. Dehghantanha, H. Karimipour, G. Srivastava, and M. Aledhari, "Enabling drones in the Internet of Things with decentralized blockchain-based security," *IEEE Internet Things J.*, vol. 8, no. 8, pp. 6406–6415, Apr. 2021.
- [5] T. Alladi, V. Chamola, R. M. Parizi, and K.-K. R. Choo, "Blockchain applications for Industry 4.0 and industrial IoT: A review," *IEEE Access*, vol. 7, no. 1, pp. 176 935–176 951, Nov. 2019.
- [6] M. Jo, K. Hu, R. Yu, L. Sun, M. Conti, and Q. Du, "Private blockchain in industrial IoT," *IEEE Netw.*, vol. 34, no. 5, pp. 76–77, Sep. 2020.
- [7] M. I. S. Assaqty, Y. Gao, X. Hu, Z. Ning, V. C. M. Leung, Q. Wen, and Y. Chen, "Private-blockchain-based industrial IoT for material and product tracking in smart manufacturing," *IEEE Netw.*, vol. 34, no. 5, pp. 91–97, Sep. 2020.
- [8] P. P. Ray, D. Dash, K. Salah, and N. Kumar, "Blockchain for IoT-based healthcare: Background, consensus, platforms, and use cases," *IEEE Syst. J.*, vol. 15, no. 1, pp. 85–94, Mar. 2021.
- [9] F. Jamil, S. Ahmad, N. Iqbal, and D.-H. Kim, "Towards a remote monitoring of patient vital signs based on IoT-based blockchain integrity management platforms in smart hospitals," *Sensors*, vol. 20, no. 8, p. 2195, Apr. 2020.
- [10] H. Lei and D. Kim, "Design and implementation of an integrated IoT blockchain platform for sensing data integrity," *Sensors*, vol. 19, no. 10, p. 2228, May 2019.
- [11] L. D. Nguyen, A. E. Kalor, I. Leyva-Mayorga, and P. Popovski, "Trusted wireless monitoring based on distributed ledgers over NB-IoT connectivity," *IEEE Commun. Mag.*, vol. 58, no. 6, pp. 77–83, Jun. 2020.
- [12] H.-N. Dai, Z. Zheng, and Y. Zhang, "Blockchain for Internet of Things: A survey," *IEEE Internet Things J.*, vol. 6, no. 5, pp. 8076–8094, Oct. 2019.
- [13] H. Lee, C. Yoon, S. Bae, S. Lee, K. Lee, S. Kang, K. Sung, and S. Min, "Multi-batch scheduling for improving performance of Hyperledger Fabric based IoT applications," in *Proc. IEEE Global Commun. Conf. (GLOBECOM)*, Waikoloa, HI, USA, Dec. 2019, pp. 1–6.
- [14] X. Xu, X. Wang, Z. Li, H. Yu, G. Sun, S. Maharjan, and Y. Zhang, "Mitigating conflicting transactions in Hyperledger Fabric-permissioned blockchain for delay-sensitive IoT applications," *IEEE Internet Things J.*, vol. 8, no. 13, pp. 10 596–10 607, Jul. 2021.
- [15] T. T. A. Dinh, R. Liu, M. Zhang, G. Chen, B. C. Ooi, and J. Wang, "Untangling blockchain: A data processing view of blockchain systems," *IEEE Trans. Knowl. Data Eng.*, vol. 30, no. 7, pp. 1366–1385, Jul. 2018.
- [16] S. Pongnumkul, C. Siripanpornchana, and S. Thajchayapong, "Performance analysis of private blockchain platforms in varying workloads," in *Proc. Int. Conf. Comput. Commun. Netw. (ICCCN)*, Vancouver, BC, Canada, Aug. 2017, pp. 1–6.
- [17] S. Wang, "Performance evaluation of Hyperledger Fabric with malicious behavior," in *Proc. Int. Conf. Blockchain (ICBC)*, San Diego, CA, USA, Jun. 2019, pp. 1–9.
- [18] M. Kuzlu, M. Pipattanasomporn, L. Gurses, and S. Rahman, "Performance analysis of a Hyperledger Fabric blockchain framework: Throughput, latency, and scalability," in *Proc. IEEE Int. Conf. Blockchain (Blockchain)*, Atlanta, GA, USA, Jul. 2020, pp. 1–5.
- [19] P. Thakkar, S. Nathan, and B. Viswanathan, "Performance benchmarking and optimizing Hyperledger Fabric blockchain platform," in *Proc. IEEE Int. Symp. Model., Anal., Simul. Comput. Telecommun. Syst. (MAS-COTS)*, Milwaukee, WI, USA, Sep. 2018, pp. 1–13.
- [20] S. Shalaby, A. A. Abdellatif, A. Al-Ali, A. Mohamed, A. Erbad, and M. Guizani, "Performance evaluation of Hyperledger Fabric," in *Proc. IEEE Int. Conf. Inform., IoT, Enabling Technol. (ICIOT)*, Doha, Qatar, Feb. 2020, pp. 1–6.
- [21] L. Foschini, A. Gavagna, G. Martuscelli, and R. Montanari, "Hyperledger Fabric blockchain: Chaincode performance analysis," in *Proc. IEEE Int. Conf. Commun. (ICC)*, Dublin, Ireland, Jun. 2020, pp. 1–6.
- [22] T. Nakaike, Q. Zhang, Y. Ueda, T. Inagaki, and M. Ohara, "Hyperledger Fabric performance characterization and optimization using GoLevelDB benchmark," in *Proc. IEEE Int. Conf. Blockchain Cryptocurrency (ICBC)*, Toronto, ON, Canada, May 2020, pp. 1–9.
- [23] T. S. L. Nguyen, G. Jourjon, M. Potop-Butucaru, and K. L. Thai, "Impact of network delays on Hyperledger Fabric," in *Proc. IEEE Int. Conf. Comput. Commun. Workshops (INFOCOM WKSHPS)*, Paris, France, Apr. 2019, pp. 1–6.
- [24] H. Sukhwani, J. M. Martinez, X. Chang, K. S. Trivedi, and A. Rindos, "Performance modeling of PBFT consensus process for permissioned blockchain network (Hyperledger Fabric)," in *Proc. Symp. Rel. Distrib. Syst. (SRDS)*, Hong Kong, China, Sep. 2017, pp. 1–3.
- [25] H. Sukhwani, N. Wang, K. S. Trivedi, and A. Rindos, "Performance modeling of Hyperledger Fabric (permissioned blockchain network)," in *Proc. IEEE Int. Symp. Netw. Comput. Appl. (NCA)*, Cambridge, MA, USA, Nov. 2018, pp. 1–10.
- [26] P. Yuan, K. Zheng, X. Xiong, K. Zhang, and L. Lei, "Performance modeling and analysis of a Hyperledger-based system using GSPN," *Comput. Commun.*, vol. 153, no. 1, pp. 117–124, Mar. 2020.
- [27] L. Jiang, X. Chang, Y. Liu, J. Misić, and V. B. Misić, "Performance analysis of Hyperledger Fabric platform: A hierarchical model approach," *Peer Peer Netw. Appl.*, vol. 13, no. 3, pp. 1014–1025, Jan. 2020.
- [28] X. Xu, G. Sun, L. Luo, H. Cao, H. Yu, and A. V. Vasilakos, "Latency performance modeling and analysis for Hyperledger Fabric blockchain network," *Inf. Process. Manag.*, vol. 58, no. 1, p. 102436, Jan. 2021.
- [29] "Hyperledger Project." [Online]. Available: <https://www.hyperledger.org>. [Accessed: 12-June-2020].
- [30] E. Androulaki, A. Barger, V. Bortnikov, C. Cachin, K. Christidis, A. D. Caro, D. Enyeart, C. Ferris, G. Laventman, Y. Manevich, S. Muralidharan, C. Murthy, B. Nguyen, M. Sethi, G. Singh, K. Smith, A. Sorniotti, C. Stathakopoulou, M. Vukolic, S. W. Cocco, and J. Yellick, "Hyperledger Fabric: A distributed operating system for permissioned blockchains," in *Proc. Eur. Conf. Comput. Syst. (EuroSys)*, Porto, Portugal, Jan. 2018, pp. 1–15.
- [31] "Hyperledger Fabric v1.3 Read the Docs." [Online]. Available: <https://hyperledger-fabric.readthedocs.io/en/release-1.3>. [Accessed: 29-Nov-2019].
- [32] D. Ongaro and J. Ousterhout, "In search of an understandable consensus algorithm," in *Proc. USENIX Ann. Tech. Conf. (ATC)*, Philadelphia, PA, USA, Jun. 2014, pp. 1–18.
- [33] J. Sousa, A. Bessani, and M. Vukolić, "A Byzantine fault-tolerant ordering service for the Hyperledger Fabric blockchain platform," in *Proc. IEEE/IFIP Int. Conf. Dependable Syst. Netw. (DSN)*, Luxembourg, Luxembourg, Jun. 2018, pp. 1–8.
- [34] "Apache Kafka." [Online]. Available: <https://kafka.apache.org>. [Accessed: 19-Apr-2021].
- [35] "Apache ZooKeeper." [Online]. Available: <https://zookeeper.apache.org>. [Accessed: 19-Apr-2021].
- [36] S. Lee, M. Kim, R.-H. Hsu, and T. Q. S. Quek, "Is blockchain suitable for data freshness? An Age-of-Information perspective," *IEEE Netw.*, vol. 35, no. 2, pp. 96–103, Mar. 2021.
- [37] C. Gorenflo, S. Lee, L. Golab, and S. Keshav, "FastFabric: Scaling Hyperledger Fabric to 20,000 transactions per second," in *Proc. IEEE Int. Conf. Blockchain Cryptocurrency (ICBC)*, Seoul, Korea (South), May 2019, pp. 1–9.
- [38] H. S. C. Thom, "A note on the gamma distribution," *Mon. Weather Rev.*, vol. 86, no. 4, pp. 117–122, Apr. 1958.
- [39] G. J. O. Jameson, "The incomplete gamma functions," *Math. Gaz.*, vol. 100, no. 548, pp. 298–306, Jul. 2016.
- [40] T. G. Bali, "The generalized extreme value distribution," *Econ. Lett.*, vol. 79, no. 3, pp. 423–427, Jan. 2003.
- [41] W. Huang, S. Xu, and S. Nnaji, "Evaluation of GEV model for frequency analysis of annual maximum water levels in the coast of United States," *Ocean Eng.*, vol. 35, no. 11, pp. 1132–1147, Aug. 2008.
- [42] F. J. Massey, Jr., "The Kolmogorov-Smirnov test for goodness of fit," *J. Am. Stat. Assoc.*, vol. 46, no. 253, pp. 68–78, Mar. 1951.
- [43] W. H. Press and S. A. Teukolsky, "Kolmogorov-Smirnov test for two-dimensional data," *Comput. Phys.*, vol. 2, no. 4, pp. 74–77, Jul. 1988.